Cluster expansion for the self-energy: A simple many-body method for interpreting the photoemission spectra of correlated Fermi systems

Claudius Gros* and Roser Valentí†
Institut für Physik, Universität Dortmund, Postfach 500 500, 4600 Dortmund 50, Germany

The self-energy of a translational invariant system of interacting fermions may be expanded in diagrams contributing to the self-energy of finite clusters with open boundary conditions. The exact solution of small clusters might therefore be used to construct a systematic approximation to the self-energy of the infinite system. This approximation incorporates both the local and the itinerant degrees of freedom on an equal footing. We develop this method for the one-band Hubbard Hamiltonian and apply it to the three-band Hamiltonian of the CuO superconductors. Already the lowest nontrivial approximation yields interesting results for the spectral density useful for the interpretation of photoemission experiments. We find (i) transfer of spectral weight from the upper to the lower Hubbard band upon doping, (ii) the formation of an *isolated* band of Zhang-Rice singlets separated from the band of triplet states by a many-body gap, and (iii) creation of density of states *above* the top of the oxygen band upon doping.

I. INTRODUCTION

Both itinerant and local degrees of freedom are important in correlated Fermi systems, such as the high-temperature superconductors, and need to be accounted for in calculations of their microscopic parameters and response functions. Since a full many-body solution is not available, theoretical studies and, consequently, interpretation of experimental data need to resort to various approximations. Band-structure calculations,[1] quantum chemical studies,[2] and small-cluster calculations[3] have been successfully used in combination with photoemission experiments[4,5] to extract[1–4] the electronic matrix elements of the CuO planes in the perovskite superconductors.[5–7] For other theoretical studies a slave-boson formulation of one-band models[8] and of the three-band Hubbard Hamiltonian[9] has been used. Studies with X operators[10] and with the unrestricted Hartree-Fock[11] and the Mori-Zwanzig projection technique[12] have been performed.

Consensus has been reached that near half-filling the so-called Zhang-Rice singlets[13–15] constitute the low-lying electronic excitations. At finite doping concentrations the situation is less clear and only impurity-type calculations[5,6] have been performed up to date. One question of both theoretical and experimental interest is the role of the oxygen bands, in particular the role of the matrix elements for hopping processes directly from one oxygen atom to another, t_{pp}, upon the nature of the states at the Fermi level. One may reformulate this question and ask why are high-temperature superconductors and heavy-fermion materials different? Here we will propose a surprising simple answer to this question. In particular we will show that for the perovskite lattice in the Mott limit (i.e., when occupation of the copper d^{10} state is suppressed) it will be just the absolute sign of t_{pp} which determines the nature of the states at the Fermi level.

We note that Green's functions obtained from the exact diagonalization of finite clusters contain in a very precise way information upon the one-particle self-energy of the infinite system. We develop then a cluster expansion for the self-energy, which (i) is exact in both the local *and* the itinerant limit and (ii) may be *systematically* improved considering larger clusters. We apply this method to the one-band and to the three-band Hubbard model. We find, already in suprisingly simple approximations, details of the one-particle density of states which we compare with results obtained from x-ray-absorption experiments.[16]

II. ILLUSTRATION: THE ONE-BAND HUBBARD MODEL

We will illustrate the method for the one-band Hubbard model in the one-site approximation. Generalization to a general many-band Hubbard model and larger clusters will then be, in principle, straightforward and discussed in detail for the case of the perovskites in the next section.

The one-band Hubbard model on a D-dimensional simple cubic lattice is given by

$$\hat{H} = t \sum_{\langle \mathbf{R},\mathbf{R}' \rangle,\sigma} \hat{c}^{\dagger}_{\mathbf{R},\sigma} \hat{c}_{\mathbf{R}',\sigma} + U \sum_{\mathbf{R}} \hat{c}^{\dagger}_{\mathbf{R},\uparrow} \hat{c}_{\mathbf{R},\uparrow} \hat{c}^{\dagger}_{\mathbf{R},\downarrow} \hat{c}_{\mathbf{R},\downarrow} . \qquad (1)$$

Here the $\hat{c}^{\dagger}_{\mathbf{R},\sigma}$ and $\hat{c}_{\mathbf{R},\sigma}$ create and/or annihilate fermions on site $\mathbf{R}$, t is the hopping matrix element between nearest-neighbor (NN) sites $\langle \mathbf{R},\mathbf{R}' \rangle$, and U is the on-site Coulomb repulsion.

We are interested in the Matsubara one-particle Green's function $G_{\mathbf{R},\sigma}(\tau) = -\langle \mathrm{T}_{\tau} \hat{c}_{\mathbf{R},\sigma}(\tau) \hat{c}^{\dagger}_{\mathbf{R},\sigma}(0) \rangle$ and

the respective spectral density, $\rho(\omega) \equiv -2\mathrm{Im}G^{\mathrm{ret}}_{\mathbf{R},\sigma}(\omega)$, where the retarded Green's function $G^{\mathrm{ret}}_{\mathbf{R},\sigma}(\omega)$ is related[17] to the Matsubara Green's function via the analytic continuation $i\omega_n \rightleftharpoons \omega + i\delta$, with $\delta = 0+$. The one-particle Green's function is given in momentum space by

$$G_{\mathbf{k},\sigma}(i\omega_n) = \frac{1}{i\omega_n + \mu - \epsilon_{\mathbf{k}} - \Sigma_{\mathbf{k},\sigma}(i\omega_n)}, \tag{2}$$

where μ is the chemical potential and $\epsilon_{\mathbf{k}}$ the one-particle dispersion relation. $G_{\mathbf{k},\sigma}(i\omega_n)$ is a function of the one-particle self-energy,

$$\Sigma_{\mathbf{k},\sigma}(i\omega_n) = \frac{1}{L^2}\sum_{\mathbf{R},\mathbf{R}'} e^{i\mathbf{k}\cdot(\mathbf{R}-\mathbf{R}')}\Sigma_{\mathbf{R},\mathbf{R}',\sigma}(i\omega_n), \tag{3}$$

where L denotes the number of sites of the lattice considered and $\Sigma_{\mathbf{R},\mathbf{R}',\sigma}(i\omega_n)$ is the sum of all irreducible diagrams contributing to the one-particle self-energy which start at site $\mathbf{R}$ and end at site $\mathbf{R}'$.

Approximations to the real-space components of the self-energy, the $\Sigma_{\mathbf{R},\mathbf{R}',\sigma}(i\omega_n)$, may be obtained by exactly diagonalizing finite clusters with open boundary conditions. Clusters with periodic boundary conditions are of no use here, since they allow for processes which may not occur on the lattice in the thermodynamic limit (for instance, propagation around the cluster). This is not the case for clusters with open boundary conditions, although there translational invariance is broken.

The real-space cluster Green's functions $G^{c}_{\mathbf{R},\sigma}(i\omega_n)$ and the respective self-energies, the $\Sigma^{c}_{\mathbf{R},\mathbf{R}',\sigma}(i\omega_n)$, are well defined and may be evaluated exactly for the cluster considered by a diagonalization routine or even analytically for some small clusters. The relation between the cluster Green's functions and self-energies is, in general, nontrivial, and we list in Appendix A these relations for some selected clusters. In any case, once we have obtained numerically (or analytically) the expressions for the $\Sigma^{c}_{\mathbf{R},\mathbf{R}',\sigma}(i\omega_n)$ we may use Eq. (2) and Eq. (3) to construct approximations for the Green's function of the extended lattice. These approximations incorporate both the local and the itinerant degrees of freedom on an equal footing, namely, both the limit $U \to 0$ and limit $t \to 0$ are recovered exactly. Furthermore, the such constructed approximations are systematic, in the sense that consideration of larger and larger clusters will eventually lead to the exact self-energy.

For concreteness, let us consider a cluster with one site $\mathbf{R}_0$ only. The exact Green's function

$$G^{1}_{\mathbf{R}_0,\sigma}(i\omega_n) = \frac{1-n_{-\sigma}}{i\omega_n + \mu} + \frac{n_{-\sigma}}{i\omega_n + \mu - U} \tag{4}$$

is related to the one-site cluster self-energy $\Sigma^{1}_{\sigma}(i\omega_n)$ via

$$G^{1}_{\mathbf{R}_0,\sigma}(i\omega_n) = \frac{1}{i\omega_n + \mu - \Sigma^{1}_{\sigma}(i\omega_n)}, \tag{5}$$

where $n_{-\sigma}$ denotes the density of particles with spin $-\sigma$. We may invert Eq. (4) and Eq. (5) and obtain

$$\Sigma^{1}_{\sigma}(i\omega_n) = \frac{n_{-\sigma}U(i\omega_n + \mu)}{i\omega_n + \mu - (1-n_{-\sigma})U} \tag{6}$$

as the first-order approximation[18] for $\Sigma_{\mathbf{R}=\mathbf{R}',\sigma}(i\omega_n)$ in Eq. (3). In this one-site cluster approximation for the self-energy $\Sigma_{\mathbf{R}\neq\mathbf{R}',\sigma}(i\omega_n) \equiv 0$. For the Green's function of the extended lattice we then obtain in this approximation

$$\begin{aligned} G_{\mathbf{k},\sigma}(i\omega_n) &= \frac{1}{i\omega_n + \mu - \epsilon_{\mathbf{k}} - \Sigma^{1}_{\sigma}(i\omega_n)} \\ &= \frac{\alpha_1(\mathbf{k})}{i\omega_n + \mu - \omega_1(\mathbf{k})} + \frac{\alpha_2(\mathbf{k})}{i\omega_n + \mu - \omega_2(\mathbf{k})}, \end{aligned} \tag{7}$$

with

$$\omega_{1,2}(\mathbf{k}) = \frac{(U+\epsilon_{\mathbf{k}})/2}{\pm\frac{1}{2}\sqrt{(U+\epsilon_{\mathbf{k}})^2 - 4(1-n_{-\sigma})U\epsilon_{\mathbf{k}}}} \tag{8}$$

and $\alpha_{1,2}(\mathbf{k}) = 1/2\,[1 \mp \{(1-2n_{-\sigma})U - \epsilon_{\mathbf{k}}\}\{(U+\epsilon_{\mathbf{k}})^2 - 4(1-n_{-\sigma})U\epsilon_{\mathbf{k}}\}^{-1/2}]$. Each Bloch state is split into two contributions, belonging to the upper and to the lower Hubbard band, respectively, as we can see from Eq. (8).

The next step is to determine the density of particles, $n_{-\sigma}$, entering Eq. (7) and Eq. (8). We have two choices: The first one is $n_{-\sigma} = (\exp[\mu/kT] + \exp[(2\mu - U)/kT])/(1 + 2\exp[\mu/kT] + \exp[(2\mu - U)/kT])$, the solution of the one-site problem. Clearly, this choice for $n_{-\sigma}$ behaves discontinuously at low temperatures T as a function of the chemical potential μ. Our approximative Green's function for the extended system, $G_{\mathbf{k},\sigma}(i\omega_n)$, would consequently be a discontinuous function of the chemical potential in a quite arbitrary way. Since we do

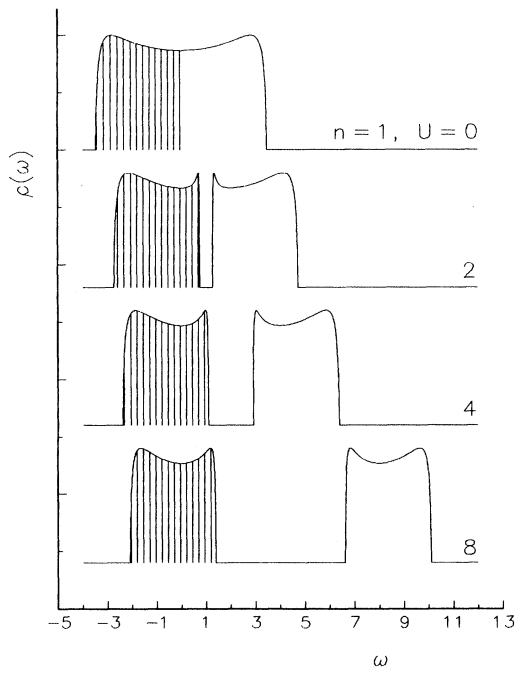

FIG. 1. Density of states, $\rho(\omega)$, for the half-filled ($n = 1$) one-band Hubbard Hamiltonian in the self-consistent one-site approximation for the self-energy and various values for $U =$ 0, 2, 4, 8 in units of t. As density of states a self-retracing path approximation for $D = 2$ has been chosen. The shaped region denotes the occupied states in the ground state. Note that the gap between the lower and the upper Hubbard bands opens for all $U > 0$.

not expect the physical solution of the system, in the thermodynamic limit, to show such a behavior, we discard this way of determining the density from the solution of the cluster under consideration.

Instead we will ask the density of particles to be determined self-consistently via

$$n_{-\sigma} = \frac{1}{L}\sum_{\mathbf{k}}\int_{-\infty}^{\infty}\frac{d\omega}{2\pi}(-2)\,\mathrm{Im}G_{\mathbf{k},-\sigma}(\omega+i\delta)\,n_F(\omega), \tag{9}$$

where $G_{\mathbf{k},-\sigma}(\omega+i\delta)$ depends itself on n_σ via Eq. (7) and $n_F(\omega)$ is the Fermi distribution function. Here we consider the paramagnetic solution with $n_\sigma = n_{-\sigma} \equiv n/2$.

At half filling, for $n = 1$, a gap of magnitude [compare Eq. (8)]

$$\sqrt{U^2+(W/2)^2} - W/2 \tag{10}$$

opens for any $U > 0$. Here the dispersion $\epsilon_{\mathbf{k}} \in [-W/2, W/2]$, with the bandwidth $W = 4D|t|$ for NN hopping. This result is valid in general for any bounded density of states, in any finite dimension.[19] We illustrate in Fig. 1 the resulting density of states for different values of U/t. For simplicity, we have chosen the $D = 2$ self-retracing path formula[21]

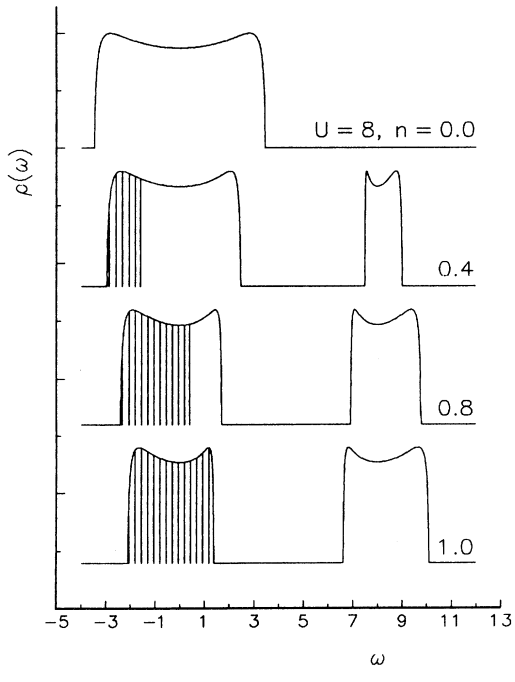

FIG. 2. Density of states, $\rho(\omega)$, for the one-band Hubbard Hamiltonian in the self-consistent one-site approximation for the self-energy at $U = 8$ in units of t and various densities $n = 0$, 0.4, 0.8, 1. As density of states a self-retracing path-approximation for $D = 2$ has been chosen. The shaded region denotes the occupied states in the ground state. Note the transfer of spectral weight from the upper to the lower Hubbard band upon doping from half-filling.

$$\rho(\epsilon') = \frac{2D}{t}\frac{\sqrt{4(2D-1)-(\epsilon'/t)^2}}{(2D)^2-(\epsilon'/t)^2}, \tag{11}$$

for the density of states (see Appendix C) when we replace $1/L\sum_{\mathbf{k}} \to \int d\epsilon'\rho(\epsilon')$ in Eq. (9). Note that the integrated density of states for both the lower and the upper Hubbard band is 1/2 per spin.

In Fig. 2 we illustrate the self-consistent density of states for $U = 8t$ for various densities of particles $n = 0$, 0.4, 0.8, 1.0. Upon doping from half filling the lower Hubbard band widens and spectral weight is transferred from the upper to the lower Hubbard band, as it has been experimentally observed for the Cu-O superconductors.[16] We conclude that the cluster-expansion method for the self-energy yields physically relevant results already in the lowest order, the one-site approximation.

III. THREE-BAND HUBBARD MODEL FOR THE PEROVSKITES

We now apply the method outlined in the previous section to the multiband Hubbard model on a two-dimensional (2D) perovskite structure appropriate for high-temperature superconductors. We take into account the three most important orbitals, the copper $d_{x^2-y^2}$ orbital and one for each oxygen in the unit cell, although the inclusion of more orbitals, such as the d_{xy}, $d_{3z^2-r^2}$, and a second oxygen orbital, would be rather straightforward. Quite a good consensus has been reached upon the parameters of this effective three-band Hubbard model. We follow Eskes and Sawatzky[6] and take (in electron notation) $\epsilon_p = 5.3$ eV for the oxygen orbital energy (we have set the zero of energy to the copper orbital energy, $\epsilon_d \equiv 0$), $t_{dp} = 1.3$ eV, and $t_{pp} = 0.65$ eV for the Cu-O and the O-O hopping matrix elements, respectively, and $U_d = 8.8$ eV for the on-site Coulomb repulsion on the copper site. We neglect all other interaction matrix elements; in particular we set $U_p = U_{dp} = 0$.

As the smallest, nontrivial cluster, we consider a central Cu site surrounded by four NN oxygen sites. Exact diagonalization of the CuO_4 cluster can be done analytically since we do not have any interaction on the oxygen sites. Only the symmetric orbital couples to the central copper sites with $t = 2t_{dp}$ being the effective matrix element.[20] The effective on-site energy of the symmetric orbital is $\epsilon = \epsilon_p + 2t_{pp}$. We then have to solve an effective two-orbital problem. The eigenstates are given in Appendix B. For the CuO_4 cluster we have only a site-diagonal self-energy on the Cu site, $\Sigma_d^{\mathrm{CuO_4}}(i\omega_n)$, which is related (see Appendix A) to the exact copper Green's function of the CuO_4 cluster, $G_d^{\mathrm{CuO_4}}(i\omega_n)$, via

$$G_d^{\mathrm{CuO_4}}(i\omega_n) = \left[i\omega_n+\mu-\Sigma_d^{\mathrm{CuO_4}}(i\omega_n)-\frac{t^2}{i\omega_n+\mu-\epsilon}\right]^{-1}. \tag{12}$$

The $\Sigma_d^{\mathrm{CuO_4}}(i\omega_n)$ determined from Eq. (12) will then serve as the approximate self-energy for the itinerant system.

As the next step we generalize the self-consistency condition Eq. (9) valid for the one-site cluster approximation to the case of larger clusters via a canonical formulation.

We may rewrite the imaginary time Matsubara Green's function as

$$G_d(\tau,\mu) = -e^{\mu\tau}\,\mathrm{Tr}\left[e^{-\beta(\hat{H}-\mu\hat{N}-\Omega)}T_\tau e^{\tau\hat{H}}\hat{d}\,e^{-\tau\hat{H}}\hat{d}^\dagger\right], \tag{13}$$

where we put explicit dependence on μ in order to stress that the trace in Eq. (13) is to be taken over the grand canonical ensemble. Here $1/\Xi \equiv \exp[\beta\Omega]$ is the grand canonical normalization constant. Site and spin indices are suppressed. In the thermodynamic limit the expectation value of $\exp[\tau\hat{H}]\,\hat{d}\,\exp[-\tau\hat{H}]\,\hat{d}^\dagger$ occurring on the right-hand side of Eq. (13) is independent of the ensemble chosen for the trace (canonical or grand canonical). For a finite cluster the choice of the ensemble makes a difference and we will choose the canonical formulation. We define the Green's function of a CuO_4 cluster with a fixed number N_c of particles by

$$G_d^{\mathrm{CuO_4}}(\tau,N_c) = -\mathrm{Tr}\left[e^{-\beta(\hat{H}-F)}T_\tau e^{\tau\hat{H}}\hat{d}\,e^{-\tau\hat{H}}\hat{d}^\dagger\right], \tag{14}$$

where the trace is over states with a fixed number N_c of particles on the CuO_4 cluster and $1/Z \equiv \exp[\beta F]$ is the canonical normalization constant.

The particle density of the cluster, n_c, is fixed via linear superposition,

$$e^{-\mu\tau}G_d^{\mathrm{CuO_4}}(\tau,\mu) = [N_c+1-L_cn_c]\,G_d^{\mathrm{CuO_4}}(\tau,N_c) + [L_cn_c-N_c]\,G_d^{\mathrm{CuO_4}}(\tau,N_c+1), \tag{15}$$

for $n_c \in [N_c/L_c,(N_c+1)/L_c]$, where L_c is number of sites of the cluster. The coefficients in Eq. (15) are chosen such that $G_d^{\mathrm{CuO_4}}(\tau,\mu)|_{n_c=(N_c+1)/L_c} = e^{\tau\mu}G_d^{\mathrm{CuO_4}}(\tau,N_c+1)$ and $G_d^{\mathrm{CuO_4}}(\tau,\mu)|_{n_c=N_c/L_c} = e^{\tau\mu}G_d^{\mathrm{CuO_4}}(\tau,N_c)$.

For the case of the high-temperature superconductors we are interested in particle densities of $n \sim 5.0$–4.7 per unit cell, corresponding to an average of $1-1.3$ holes per unit cell (note that the unit cell corresponds formally to a CuO_2 cluster with three orbitals). For the cluster approximation to the copper self-energy we consider the CuO_4 cluster which contains three nonbonding oxygen orbitals in addition to the hybridized bonding and antibonding orbitals. Since the three nonbonding orbitals of the CuO_4 clusters are inert (and occupied), we need to consider, for the calculation of the copper Green's function, the bonding and the antibonding orbitals only (which we call the "effective two-orbital" problem). We solve the effective two-orbital problem for a total of $N_c = 2$ and $N_c+1 = 3$ particles, corresponding to the situation with two or one holes per unit cell, respectively, in Eq. (15). Having determined $G_d^{\mathrm{CuO_4}}(i\omega_n)$ from Eq. (15) we obtain $\Sigma_d^{\mathrm{CuO_4}}(i\omega_n)$ from Eq. (12) and finally the full Green's function by replacing $\epsilon_d \to \epsilon_d + \Sigma_d^{\mathrm{CuO_4}}(i\omega_n)$ in the band Green's function of the extended CuO plane [see Eq. (C1) and Eq. (C6) in Appendix C and next paragraph]. The average density $n \equiv n_c$ entering Eq. (15) is determined via the self-consistency condition Eq. (9).

For the band Green's function we have used, for numerical simplicity, a self-retracing path approximation, which is highly accurate for the perovskite lattice (see Appendix C). In Fig. 3 we illustrate the partial oxygen and the partial copper density of states. The pure oxygen band ($t_{dp}=0$, $t_{pp}=0.65$) has a larger bandwidth than the band with $t_{dp}=1.3$, $t_{pp}=0.0$, but nevertheless the states at the top of the full band ($t_{dp}=1.3$, $t_{pp}=0.65$) are fully hybridized. This result depends crucially on the absolute sign of t_{pp} being positive. In Fig. 4 we present the results for the oxygen and copper density of states for the hypothetical case $t_{pp}<0$ (we did choose $\epsilon_p = 6.3$ eV). The states at the top of the band are of nonbonding oxygen character. In the Mott-Hubbard or charge-transfer limit (i.e., with the copper orbital only half-filled and occupation of the copper d^{10} configuration suppressed), doping would occur into these nonbonding oxygen orbitals and the resulting state would be completely different, resembling more the Kondo-lattice model.

Also note the singularity $\sim |\omega+\mu-\epsilon_p|^{-1/3}$ in Fig. 3 at $\omega' = \epsilon_p = 5.3$ eV. This singularity is a precursor of the logarithmic Van Hove singularity of the true two-dimensional band (with a cosinus dispersion relation). It is quite remarkable that the self-retracing path approximation for the perovskites, which does sum up the lowest-order loops around the copper sites *exactly* (see Appendix C), starts describing this Van Hove singularity. Note that no indication of the Van Hove singularity in two or higher dimensions can be found in the standard self-retracing path approximation [compare Fig. 3 with Eq. (11) and Fig. 2].

In Figs. 5 and 6 we present for various values of the hole doping $x = 0,\ 0.1,\ 0.2,\ 0.3$ our results for the copper and the oxygen density of states obtained from the full Green's function (solid line) with the self-energy determined via the effective two-orbital approximation at zero temperature, as described above. The respective positions of the chemical potential are indicated by the vertical arrows. For comparison we also show in Fig. 5

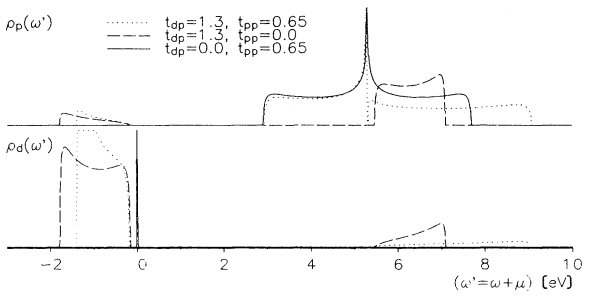

FIG. 3. Oxygen and copper density of states, $\rho_p(\omega)$ and $\rho_d(\omega)$, for the three-band Hamiltonian of the CuO-planes with no interaction, $U_d = 0$, as a function of $\omega' = \omega+\mu$. Shown is the density of states of the hybridized bands (dotted line), for the band with $t_{pp}=0$ (dashed line), and for the pure oxygen band (solid line) with a singularity of Van Hove type at $\epsilon_p = 5.3$ eV. Note the relative bandwidths. The nonbonding oxygen orbitals lie (since $t_{pp}>0$ for the perovskites) in between $\omega' \sim (3, 5.3)$ eV (dotted and solid lines). For $t_{pp}<0$ they would be located at the top of the band (see Fig. 4).

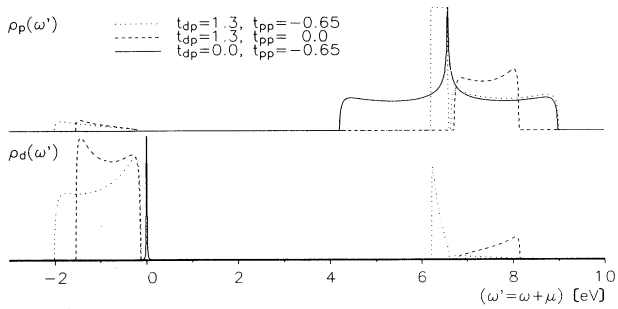

FIG. 4. Oxygen and copper noninteracting density of states, $\rho_p(\omega)$ and $\rho_d(\omega)$, for the hyphothetical case $t_{pp} < 0$ ($\epsilon_p = 6.3$ eV, $U_d = 0$). Shown is the density of states of the hybridized bands (dotted line), for the band with $t_{pp} = 0$ (dashed line), and for the pure oxygen band (solid line). Note that the states at the top of the band are of nonbonding oxygen character (dotted line) and that for large U_d doping would occur into these nonbonding orbitals leading to a Kondo-type model.

the pure band density of states (dotted line), i.e., the result for $U_d = 0$ and the positions and the weights of the δ peaks contributing to the density of states of a single CuO_4 cluster. For dopings $x > 0$ some more peaks appear due to the contribution of $G_d^{CuO_4}(\tau, N_c = 2)$ to

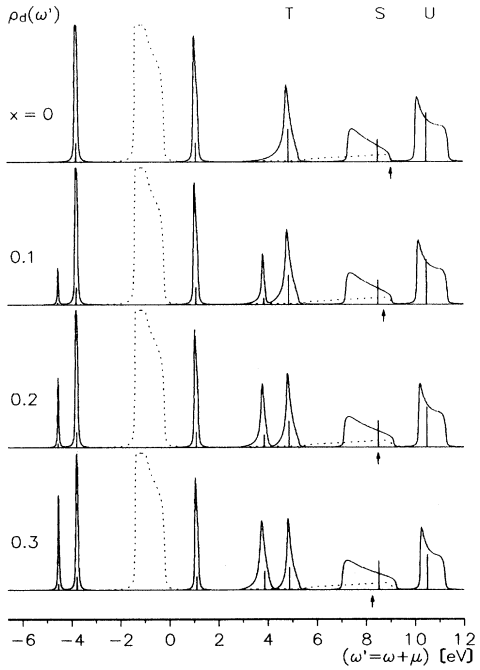

FIG. 5. Copper density of states, $\rho_d(\omega' = \omega + \mu)$, for various hole dopings $x = 0$, 0.1, 0.2, 0.3 and $U_d = 0$ (dotted line) and for $U_d = 8.8$ (solid line) in the effective two-orbital approximation for the self-energy. The respective position of the chemical potential is indicated by the arrows. T, S, and U denote the Zhang-Rice triplet, singlet, and the upper copper Hubbard band, respectively. Also shown are the positions and the weights of the δ peaks of a single CuO_4 cluster. Note the transfer of spectral weight from $\omega \sim (-2, 0)$ of the hybridized band to higher energies due to the interaction.

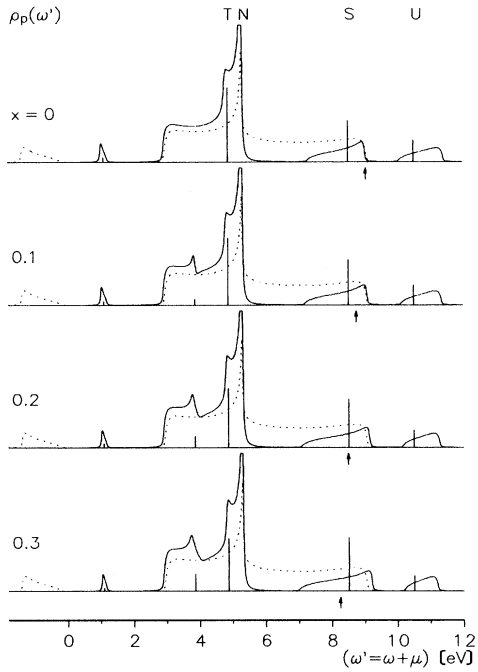

FIG. 6. Oxygen density of states, $\rho_p(\omega' = \omega + \mu)$, for various hole dopings $x = 0$, 0.1, 0.2, 0.3 and $U_d = 0$ (dotted line) and for $U_d = 8.8$ (solid line) in the effective two-orbital approximation for the self-energy. The respective position of the chemical potential is indicated by the arrows. T, S, U, and N denote the Zhang-Rice triplet, singlet, the upper copper Hubbard band, and the nonbonding oxygen orbitals, respectively. Also shown are the positions and the weights of the δ-peaks of a single CuO_4 cluster. Note that the singlet states form a separate many-body band and that spectral weight above the top of the noninteracting band is created upon doping.

Eq. (15); in particular we observe the strong growth of an additional peak about 1 eV below the Zhang-Rice triplet state upon doping.

The interaction does drastically affect the density of states. The density of states of the copper band, $\rho_d(\omega' = \omega + \mu)$, is completely suppressed for $\omega' \sim (-1.5, 0)$ and transferred partially to lower and partially to higher energies (see Fig. 5). The nonbonding oxygen orbitals are, on the other hand, neither affected by U_d nor do they hybridize with the peak at $\omega = 3.86$ eV occurring for finite doping, $x > 0$ (see Fig. 6). The Zhang-Rice singlet shows up in the peak of the CuO_4 cluster at $\omega' = 8.51$ eV, which happens to lie near to the top of the noninteracting band. The Zhang-Rice singlet hybridizes strongly with the top of the noninteracting band since $t_{pp} > 0$, as we discussed above. The singlet band is separated from the copper upper Hubbard band by the charge-transfer gap and, as a new result, also from the triplet band. The suppression of the density of states in between the triplet and the singlet bands is a typical many-body effect due to the translational invariance and the total sum rule for the spectral weight. This effect, which is similar to the one which leads to the formation of a separate upper Hubbard band in the context of the one-band Hubbard

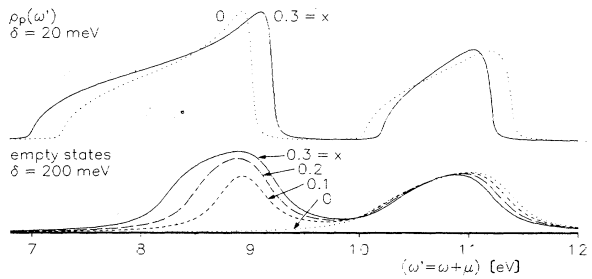

FIG. 7. Oxygen density of states [$\rho_p(\omega' = \omega + \mu)$, top] and the empty states (bottom), for various hole-dopings $x = 0$, 0.1, 0.2, 0.3. Upon doping the true position of the lower peak shifts to higher energies (top), though a limited experimental resolution of $\delta = 200$ meV [see paragraph above Eq. (2)] might show a shift to lower energies (bottom), due to the asymmetry of the band.

model (see Fig. 1), could not be observed in an impurity calculation.[6]

At half filling the former top of the noninteracting band coincides exactly with the top of the many-body valence band, but upon doping density of states is created *above* the top of the noninteracting band. This is an conspicuous consequence of the many-body nature of the singlet states as a band of antibound states. The integrated weight of the upper band, located around $\omega' = 10.52$ eV, decreases more or less proportionally to the doping, i.e., by about 30% for $x = 0.3$.

In Fig. 7 we present the oxygen spectral weight $\rho_p(\omega' = \omega + \mu)$ for energies around the position of the chemical potential. We also show the results for the empty states, i.e., $\rho_p(\omega')[1 - n_F(\omega')]$, with the inclusion of broadening effects of magnitude $\delta = 200$ meV. A straightforward comparison of this curve with x-ray-absorption experiments around the oxygen K edge[16] is not possible, since we did not include excitonic effects, which would change the position of the peak at higher energy. Nevertheless, the evolution of the peak at lower energy (corresponding to the singlet states) with doping compares well with the experiment, but the reduction of the spectral weight of the peak at higher energy is not nearly as pronounced as the one seen experimentally and in simulations by a one-band Hamiltonian with inclusion of excitonic effects.[16] We find, similar to the results for the one-band Hubbard model (compare Fig. 2), a reduction of the spectral weight of the upper Hubbard band proportional only to the amount of doping, which is barely discernible in Fig. 7. We therefore conclude that the results for the empty states presented in Fig. 7 would not differ drastically when doping into a band insulator would be considered and that the inclusion of final-state interactions –the excitonic effects discussed by Chen *et al.*[16]— are important in order to explain the observed drastic reduction of the weight in the upper Hubbard band.

IV. CONCLUSIONS

We have shown that it is always possible to expand the self-energy of an interacting, translational invariant system in terms of the exact solution of clusters with a finite number of sites. Then a systematic cluster expansion is obtained which (i) converges to the exact solution for large enough clusters and (ii) treats the local and the itinerant degrees of freedom on a equal footing. This method allows one to make use of present computational possibilities by extracting a self-energy of the *itinerant* system from the results of exact diagonalization studies of finite clusters.

We applied the cluster-expansion method for the self-energy to the case of the one-band Hubbard Hamiltonian and to the three-band Hamiltonian appropriate for the CuO planes of the high-temperature superconductors. We showed that already the smallest clusters, namely, the one-site cluster and the effective two-orbital cluster, are good approximations and yield very interesting results for the one-band and the three-band Hamiltonians, respectively. In particular, the transfer of spectral weight from the upper to the lower Hubbard band is found naturally in these approximations.

For the case of the CuO superconductors we find that the band of singlet states at the Fermi level is separated by a gap from the rest of the oxygen band, in particular from the triplet states, due to an effect similar to the one which leads to the formation of a separate upper Hubbard band for the one-band Hubbard Hamiltonian. We find in addition that the singlet states create spectral weight *above* the oxygen band upon doping, due to the formation of a translational invariant antibound state (in electron notation).

ACKNOWLEDGMENTS

We would like to thank W. Weber for discussions. This work was supported by the Deutsche Forschungsgemeinschaft and by the Minister für Wissenschaft und Forschung des Landes Nordrhein-Westfalen. Part of the numerical calculations were done at the Hochleistungs Rechenzentrum Jülich.

APPENDIX A: RELATION BETWEEN SELF-ENERGIES AND GREEN'S FUNCTION FOR SOME SMALL CLUSTERS

The numerical or analytical solution of a Hamiltonian of Hubbard type on a small cluster with open boundary conditions allows to obtain the exact Green's functions of the cluster. The processes contributing to these cluster Green's functions are a subset of the processes contributing to the Green's functions of the extended system, a relation which holds also for their respective self-energies. These self-energies are defined as irreducible with respect to the noninteracting Green's functions, which incorporate only the kinetic energy.

As an intermediate step we consider the cluster Green's function graphically in terms of an expansion around the chemical potential, i.e., with

$$G_i^{(0)}(i\omega_n) = 1/x_i, \quad x_i = i\omega_n + \mu - \epsilon_i, \tag{A1}$$

as the unperturbed Green's function on site i, where we have included an on-site energy ϵ_i. In terms of this ex-

pansion around the chemical potential the cluster self-energies $\Sigma_{i,j}$, are defined as sums of all processes which do not contain a $G_i^{(0)}$ line which may be cut. By comparing the corresponding Dysons equations, we find the relationships

$$\begin{array}{ll} \Sigma_{i,j} = \Sigma^c_{i,j} & \text{for } (i,j) \text{ not NN}, \\ \Sigma_{i,j} = t + \Sigma^c_{i,j} & \text{for } (i,j) \text{ NN}, \end{array} \tag{A2}$$

between the cluster self-energy in terms of an expansion around zero, $\Sigma_{i,j}$, and the cluster self-energy in terms of an expansion around the kinetic energy, $\Sigma^c_{i,j}$, which are then our approximation for the self-energies of the extended system.

We now note that Dyson's equation in terms of the $G_i^{(0)}$ and the various $\Sigma_{i,j}$ is equivalent to a generalized tight-binding problem with "on-site energies" $\Sigma_{i,i}$ and "hopping matrix elemets" $\Sigma_{i\neq j}$, which may be summed up.

Two-site cluster. For a two-site cluster (or *two-orbital* cluster) we have $\Sigma_{1,1}$, $\Sigma_{2,2}$, and $\Sigma_{1,2} = \Sigma_{2,1}$. The relations are

$$\begin{aligned} G^c_{1,1} &= \left[x_1 - \Sigma_{1,1} - \Sigma_{1,2}\tfrac{1}{x_2-\Sigma_{2,2}}\Sigma_{2,1}\right]^{-1}, \\ G^c_{1,2} &= G^c_{1,1}\Sigma_{1,2}\tfrac{1}{x_2-\Sigma_{2,2}}, \end{aligned} \tag{A3}$$

with analogous equations for $G^c_{2,2}$ and $G^c_{2,1} = G^c_{1,2}$. Given the exact cluster Green's functions, the $G^c_{i,j}$, one needs to invert Eq. (A3) and obtains, with help of Eq. (A2), the two-site approximations for the self-energy of the extended system, the $\Sigma^c_{i,j}$.

For the symmetric two-site cluster, with $\Sigma_{1,1} = \Sigma_{2,2} \equiv \Sigma_0$, $x_1 = x_2 \equiv x$, and $\Sigma_{1,2} \equiv \Sigma_1$, Eq. (A3) may be also obtained by considering the Fourier components of this effective tight-binding problem,

$$\begin{aligned} G^c_{1,1} &= \tfrac{1}{2}\left[\tfrac{1}{x-\Sigma_0-\Sigma_1} + \tfrac{1}{x-\Sigma_0+\Sigma_1}\right], \\ G^c_{1,2} &= \tfrac{1}{2}\left[\tfrac{1}{x-\Sigma_0-\Sigma_1} - \tfrac{1}{x-\Sigma_0+\Sigma_1}\right]. \end{aligned} \tag{A4}$$

Similarly we find for the case of no interaction on site 2, i.e., with $\Sigma_{1,2} = t$, $\Sigma_{1,1} = \Sigma^c_{1,1}$, $\Sigma_{2,2} = 0$, so that $G^c_{1,1} = (x_1 - \Sigma^c_{1,1} - t^2/x_2)^{-1}$, leading to Eq. (12).

Three-site cluster. The $(n+1)$-site cluster with one central site and its n equivalent NN sites can be easily done considering the star of NN sites as a one-dimensional finite ring and a decomposition into Fourier components. For the case of the three-site cluster we have the on-site self-energies $\Sigma_{0,0}$, $\Sigma_{1,1} = \Sigma_{2,2}$ for the central site and its NN, respectively, and the off-site self-energies $\Sigma_{0,1} = \Sigma_{0,2}, \Sigma_{1,2}$. The symmetric-antisymmetic combination of the orbitals on sites 1 and 2 has the effective on-site energies $\Sigma_s \equiv \Sigma_{1,1} + \Sigma_{1,2}$ and $\Sigma_a \equiv \Sigma_{1,1} - \Sigma_{1,2}$, respectively. We find

$$\begin{aligned} G^c_{0,0} &= \left[x_0 - \Sigma_{0,0} - \Sigma_{0,1}\tfrac{2}{x_1-\Sigma_s}\Sigma_{1,0}\right]^{-1}, \\ G^c_{1,1} &= \tfrac{1}{2}\left[G^c_{1,1} + G^c_{2,2}\right] = \tfrac{1}{2}\left[G^c_{s,s} + G^c_{a,a}\right] \\ &= \tfrac{1}{2}\left[x_1 - \Sigma_s - \Sigma_{1,0}\tfrac{2}{x_0-\Sigma_{0,0}}\Sigma_{0,1}\right]^{-1} \\ &\quad + \tfrac{1}{2}\left[x_1 - \Sigma_a\right]^{-1}, \end{aligned} \tag{A5}$$

and similar equations for $G^c_{0,1}$ and $G^c_{1,2}$.

APPENDIX B: EIGENSTATES OF THE CuO_4 CLUSTER

The dynamics of the CuO_4 cluster corresponds to an effective two-orbital problem since the nonbonding oxygen orbitals do not couple to the central copper site. In this effective two-orbital model the d site has an on-site energy ϵ_p (which we set to zero) and an on-site Coulomb repulsion $U_d = 8.8$ eV. The parameters of the p site are $\epsilon = \epsilon_p + 2t_{pp} = 6.6$ eV and $U_p = 0$. The effective hybridization matrix element is $t = 2t_{dp} = 2.6$ eV, all in electron notation. The eigenstates are

$$\begin{aligned} |1,i,\sigma\rangle &= \left(a_i \hat{d}^\dagger_\sigma + b_i \hat{p}^\dagger_\sigma\right)|0\rangle, \\ |2,T,\sigma\rangle &= \hat{d}^\dagger_\sigma \hat{p}^\dagger_\sigma |0\rangle, \\ |2,T,0\rangle &= 2^{-1/2}\left(\hat{d}^\dagger_\uparrow \hat{p}^\dagger_\downarrow - \hat{p}^\dagger_\uparrow \hat{d}^\dagger_\downarrow\right)|0\rangle, \\ |2,S,j\rangle &= \left(a_j \hat{d}^\dagger_\uparrow \hat{d}^\dagger_\downarrow + b_j/\sqrt{2}[\hat{d}^\dagger_\uparrow \hat{p}^\dagger_\downarrow + \hat{p}^\dagger_\uparrow \hat{d}^\dagger_\downarrow] + c_j \hat{p}^\dagger_\uparrow \hat{p}^\dagger_\downarrow\right)|0\rangle, \\ |3,i,\sigma\rangle &= \left(a_i \hat{d}^\dagger_\sigma + b_i \hat{p}^\dagger_\sigma\right)\hat{d}^\dagger_{-\sigma}\hat{p}^\dagger_{-\sigma}|0\rangle, \\ |4,S,0\rangle &= \hat{d}^\dagger_\uparrow \hat{d}^\dagger_\downarrow \hat{p}^\dagger_\uparrow \hat{p}^\dagger_\downarrow]|0\rangle, \end{aligned}$$

where the a_i, b_i $(i = 1,2)$ and the a_j, b_j, c_j $(j = 1,2,3)$ are coefficients to be determined. T and S stand for *triplet* and *singlet*, respectively. The energies $\epsilon(1,i,\sigma)$ of the one-particle states $|1,i,\sigma\rangle$ and the energies $\epsilon(3,\{i=1,2\},\sigma)$ of the three-particle states $|3,i,\sigma\rangle$ are given, respectively, by the eigenvalues of

$$\begin{pmatrix} 0 & t \\ t & \epsilon \end{pmatrix}, \qquad \begin{pmatrix} \epsilon + U_d & t \\ t & 2\epsilon \end{pmatrix}. \tag{B1}$$

The energies of the triplet states are $\epsilon(2,T,\sigma) = \epsilon(2,T,0) = \epsilon$ and the energies $\epsilon(2,S,j)$ of the three singlet states are given by the eigenvalues of

$$\begin{pmatrix} U_d & \sqrt{2}t & 0 \\ \sqrt{2}t & \epsilon & \sqrt{2}t \\ 0 & \sqrt{2}t & 2\epsilon \end{pmatrix}, \tag{B2}$$

which can be found using Cardano's formulas. The state with the lowest eigenvalue corresponds then to the Zhang-Rice singlet. Finally $\epsilon(4,S,0) = U_d + 2\epsilon$ corresponds to a state in the upper Hubbard band. Once the eigenvalues and the eigenstates have been determined, the cluster Green's function Eq. (14) may be calculated using Lehmann's representation.

APPENDIX C: SELF-RETRACING PATH APPROXIMATION FOR PEROVSKITES

Here we derive the formulas for the density of states to be used in the self-consistency Eq. (9) for the case of the Cu-O planes. For numerical simplicity we use a generalized self-retracing path approximation.[21] We set $x_d \equiv i\omega_n + \mu - \epsilon_d$ and $x_p \equiv i\omega_n + \mu - \epsilon_p$. We define a band self-energy Σ_p for the copper and the oxygen Green's functions via

$$\begin{aligned} G_d &= \left[x_d - \tfrac{Zt^2_{dp}}{x_p-\Sigma_p}\right]^{-1}, \\ G_p &= \left[x_p - 2\Sigma_p\right]^{-1}, \end{aligned} \tag{C1}$$

where $Z = 2D$ is the coordination number.

We discuss first the case $t_{pp} = 0$, which is simpler. In this case the band self-energy is determined from

$$\Sigma_p = t_{dp}^2 \left[x_d - \frac{(Z-1)t_{dp}^2}{x_p - \Sigma_p} \right]^{-1}, \tag{C2}$$

with the solution

$$2\Sigma_p = x_p - (Z-2)t_{dp}^2/x_d - \sqrt{(x_p - (Z-2)t_{dp}^2/x_d)^2 - 4t_{dp}^2 x_p/x_d}, \tag{C3}$$

where the sign in front of the square root has been chosen such that $\Sigma - p$ vanishes in the limit $t_{dp} \to 0$. In one dimension, for $Z = 2$, the self-retracing path approximation [Eq. (C3)] together with Eq. (C1) is exact.[21] In two dimensions, for $Z = 4$, the four band edges of the bonding-antibonding band (given by the zeros of the square root) are

$$x_p/2 \pm \sqrt{(x_p/2)^2 + 4t_{dp}^2(1 \pm \sqrt{3/4})} \tag{C4}$$

and are very close to the exact result[15]

$$x_p/2 \pm \sqrt{(x_p/2)^2 + 4t_{dp}^2(1 \pm 1)}. \tag{C5}$$

The general case $t_{pp} \neq 0$ is more complex. In order to obtain a recursion formula for Σ_p similar to Eq. (C3) we consider a CuO_4 cluster via an equation-of-motion technique. We then find

$$\Sigma_p = (x_p - \Sigma_p)\, y\, /(x_p - \Sigma_p - y), \tag{C6}$$
$$y = t_{dp}^2/x_d + 2(t_{pp} + t_{dp}^2/x_d)^2/(x_p - \Sigma_p - 2t_{dp}^2/x_d),$$

which might be solved recursively. Note that the absolute sign of t_{pp} enters Eq. (C6). The interacting Green's function for the perovskites will be obtained by replacing $x_d \to i\omega_n + \mu - \Sigma_d^{CuO_4}(i\omega_n)$ in Eq. (C6) and Eq. (C1) with $\Sigma_d^{CuO_4}(i\omega_n)$ determined from Eq. (12).

For $t_{pp} = 0$, Eq. (C6) reduces to Eq. (C3). For $t_{dp} = 0$, Eq. (C6) becomes

$$\Sigma_p(x_p - \Sigma_p)^2 = 2t_{pp}^2 x_p, \tag{C7}$$

which might be solved with Cardano's formulas. Note that Eq. (C7) is *not* identical to that of the standard self-retracing path approximation[21] (though the net of oxygens connected by t_{pp} do form a simple 2D square lattice) given in Eq. (11) since part of the loops around plaquettes are summed. The self-energy becomes purely real for $x_p > \sqrt{27/2}\, t_{pp} \sim 3.6742\, t_{pp}$. This band edge is above the one obtained by the standard self-retracing path approximation $2\sqrt{2D-1} \sim 3.464$ in 2D. The resulting density of states, illustrated in Fig. 3, has a pole of type $|x_p|^{-1/3}$, as one can easily show, which is a precursor of the logarithmic Van Hove singularity in 2D.

---

*Electronic address: UPH301 at DDOHRZ11
†Electronic address: UPH084 at DDOHRZ11

[1] L. F. Matheiss, Phys. Rev. Lett. **58**, 1028 (1987); M. S. Hybertsen, M. Schlüter, and N. E. Christensen, Phys. Rev. B **39**, 7247 (1989).
[2] A. K. McMahan, J. F. Annett, and R. M. Martin, Phys. Rev. B **42**, 6268 (1990); J. B. Grant and A. K. McMahan, *ibid.* **46**, 8440 (1992).
[3] W. Stephan and P. Horsch, Phys. Rev. Lett. **66**, 2258 (1991); H. Eskes, M. M. J. Meinders, and G. A. Sawatzky, *ibid.* **67**, 1035 (1991); E. Dagotto, A. Moreo, F. Ortolani, J. Riera, and D. J. Scalapino, *ibid.* **67**, 1918 (1991); G. Dopf, J. Wagner, P. Dietrich, A. Muramatsu, and W. Hanke, *ibid.* **68** 2082 (1992); Y. Ohta, T. Tsutsui, W. Koshibae, T. Shimozato, and S. Maekawa, Phys. Rev. B **46**, 14022 (1992).
[4] A. Fujimori *et al.*, Phys. Rev. Lett. **35**, 8814 (1987); R. List *et al.*, Phys. Rev. B **38**, 11966 (1989); T. Takahashi *et al.*, *ibid.* **39**, 6636 (1989); A. J. Arko *et al.*, *ibid.* **40**, 2268 (1989); C. Olson *et al.*, *ibid.* **42**, 381 (1990); J. Campuzano *et al.*, Phys. Rev. Lett. **64**, 2308 (1990); R. Liu *et al.*, Phys. Rev. B **46**, 11056 (1992).
[5] O. Gunnarson *et al.*, Phys. Rev. B **41**, 4811 (1990).
[6] H. Eskes, L. H. Tjeng, and G. A. Sawatzky, *ibid.* **41**, 288 (1990); H. Eskes and G. A. Sawatzky, Phys. Rev. B **44**, 9656 (1991).
[7] F. Mila, Phys. Rev. B **38**, 11358 (1988).
[8] H. Chi and A. D. S. Nagi, Phys. Rev. B **46**, 421 (1992); C. Castellani *et al.*, Phys. Rev. Lett. **69**, 2009 (1992).
[9] P. Entel and J. Zielinski, Phys. Rev. B **42**, 307 (1990); J. Schmalian, G. Baumgärtel, and K.-H. Bennemann, Phys. Rev. Lett. **68**, 1406 (1992).
[10] M. H. Sasaki, H. Matsumoto, and M. Tachiki, Phys. Rev. B **46**, 3022 (1922).
[11] M. P. López Sancho, J. Rubio, M. C. Refolio, and J. M. López Sancho, Phys. Rev. B **46**, 11110 (1992).
[12] A. J. Fedro, Y. Zhou, T. C. Leuny, B. N. Harmon, and S. K. Sinha, Phys. Rev. B **46**, 14785 (1992).
[13] F. C. Zhang and T. M. Rice, Phys. Rev. B **37**, 3759 (1988); F. C. Zhang, *ibid.* **39**, 7375 (1989).
[14] C.-X. Chen, H.-B. Schüttler, and A. J. Fedro, Phys. Rev. B **41**, 2581 (1990); S. B. Bacci *et al.*, *ibid.* **44**, 7504 (1991).
[15] R. Valentí and C. Gros, Z. Phys. B **90**, 161 (1993).
[16] H. Romberg *et al.*, Phys. Rev. B **42**, 8768 (1990); C. T. Chen *et al.*, Phys. Rev. Lett. **66**, 104 (1991).
[17] G. D. Mahan, *Many-Particle Physics* (Plenum, New York, 1981).
[18] J. Hubbard, Proc. R. Soc. London A **276**, 238 (1963); **277**, 238 (1964); **281**, 401 (1964).
[19] In the limit of infinite dimensions, $D \to \infty$, with the usual scaling $t \to t^*/\sqrt{2D}$, the gap at half filling does close for all ratios of U/t^*.
[20] The factor of 2 in the formula $t = 2t_{dp}$ for the effective matrix element comes from the normalization $\sqrt{4} = 2$ constant for the symmetric combination of the four oxygen orbitals surrounding a central copper site.
[21] W. E. Brinkman and T. M. Rice, Phys. Rev. B **2**, 1324 (1970).